Activated barrier crossing of macromolecules at a submicron-size entropic trap

Alok K. R. Paul
Max Planck Institute for Polymer Research, Ackermannweg 10, D-55128 Mainz, Germany
(Received 11 July 2005; published 14 December 2005)

We study the thermally activated barrier crossing by long chain molecules, initially confined to one side of an entropic trap. The entropic barrier is assumed to be of Kramers type. The barrier width is considered to be larger than the chain. The latter is in turn assumed to be long enough, so that a continuum description of the chain is applicable throughout the space. The barrier crossing rate is calculated using multidimensional Kramers theory and the functional integral method. For chains having the same total number of segments, the activation energy itself remains constant. However, the preexponential factor depends on the structure of the polymer. Polymers with the same molecular weight but having longer arms can effect larger fluctuations, thereby increasing its chance to cross the barrier. This leads to an almost exponential increase of the rate prefactor with the radius of gyration. The difference in the barrier crossing rates could be effectively exploited for the separation of molecules having architectural differences, for example, DNA of same length but different degrees of supercoiling. This is illustrated by considering star polymers. The Rouse-Ham model is used to analyze the mechanism of the barrier crossing. We show how the rate expression of the Arrhenius type is affected by the long arms of the star chain.

DOI: 10.1103/PhysRevE.72.061801 PACS number(s): 61.41.+e, 05.40.−a, 83.10.Mj, 87.15.He

I. INTRODUCTION

Electrophoresis and gel permeation chromatography [1] are standard methods of separation of polymers and DNA by length. These processes exploit size dependent differences in the time it takes for the molecules to migrate through a random porous network. Small molecules are thought to adopt an approximately spherical conformation [2] while larger molecules are forced to snake through [3–5] the gel media. Molecules of intermediate size can get temporarily trapped in the pores, where the molecule can extend and thus maximize its conformational entropy. The molecules migrate by diffusing from one pore to another and thus pass through regions where they cannot sample all the conformations. Hence each time the molecules go from one pore to another they have to overcome an entropic barrier. An interesting recent study [6] reports the effect of entropic trapping on the diffusion rate for molecules of different sizes.

As the length of the chains becomes longer, the efficiency of the separation process deteriorates seriously. Recently a well defined nanofluidic channel device, consisting of many entropic traps, was introduced [7] to overcome this limitation. The device, see Fig. 1, consists of narrow constrictions and wider regions that cause size-dependent trapping of DNA at the constrictions. The process creates mobility differences, thus enabling efficient separation of long DNA molecules (5000 to 160 000 base pairs). In a Brownian dynamics simulation, Streek *et al.* [8] reproduced the experimental condition [7] of the nanofluidic device and found that the mobility increases with the length of the chain. They also find that smaller molecules have a higher probability to remain trapped in regions of low electric field. Tessier *et al.* [9] performed computer simulation studies of the device where the driving force is a varying (ac) field in the zero frequency limit. They find that a time-asymmetric pulse can yield bidirectional transport for different molecular sizes. At finite frequency they uncover a resonance for the molecular velocity in the channel which could lead to improved performance.

In all these studies a polymer undergoes an activated barrier crossing at a submicron sized constriction. Similar techniques can be used for long chain molecules with different architectures. The architectural difference involves considerable differences in their dynamics. For example, plasmid DNA is made up of two covalently closed circular strands which are normally found in compact supercoiled form [10]. Isolation steps, like nicking by nucleases, chemical treatment, or mechanical shear, can introduce breaks in the strands which allow the DNA to relax and form an open circular form [10] or other forms with lesser degree of supercoiling [11]. Separation of these forms often needs special techniques [12,13]. However, a detailed study of these diverse kind of polymers diffusing through a gel or an array of entropic traps is still lacking.

The focus of this paper lies in solving the thermally activated escape of a flexible polymer over a barrier. With the chain being viewed as a coupled array of Brownian particles, each subjected to the space fixed potential, the problem is a generalization of the well known Kramers theory to many degrees of freedom [14]. We consider a chain with simple harmonic coupling between neighboring segments and assume the entropic barrier of the Kramers type [15]; see Sec. II for details. The model will be appropriate for a situation where the barrier curvature is small on microscopic scales so that the extension of individual segments remains small throughout the dynamics of the chain. The barrier width is

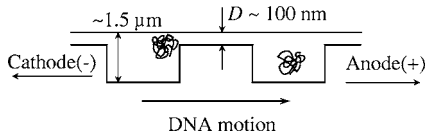

FIG. 1. A cross section of the nanofluidic device with entropic barriers.

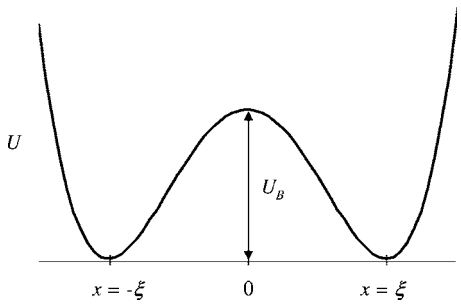

FIG. 2. The potential energy per segment of the chain, plotted as a function of the position.

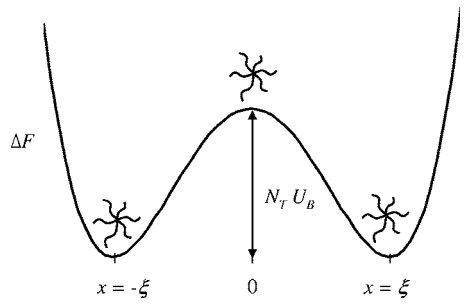

FIG. 3. The free energy landscape for the barrier crossing process. Note that the star chain is smaller than the width of the potential. The star is assumed to be initially trapped in the potential well at $x=-\xi$.

considered large enough so that the escape process is dominated by the activation of the entire polymer over the barrier. These conditions can be easily reproduced in the experiments; the barrier parameters are related with different experimental situations. In this case, the activation energy is proportional to the total number of monomers in the chain. Using multidimensional Kramers theory [16–18] an analytical expression of the barrier crossing rate is obtained.

To illustrate the role of the architectural differences we consider multiarm star polymer as a model system. The star configuration [19,20] is interesting because it gives rise to motional modes extending over different arms of the macromolecule. Further, the multiplicity of arms also leads to degeneracy of the modes. These modes have a significant effect on the rates of barrier crossing. The aim in this paper is to present these results of the escape process.

Throughout the work use is made of the multiarm star polymer. This is no limitation, if one is concerned with a barrier crossing process which is dominated by the activation of the entire polymer over the barrier. The conclusions are general and applicable to macromolecules of any architecture. On the other hand, if one is interested in the activated barrier crossing process where the width of the barrier is small compared to the size of the macromolecule [21], one has to consider the contribution of all paths leading to the other side of the barrier. This, at present, seems rather involved. However, we believe that the star polymers capture the essential physics of the problem.

II. THE MODEL

A. The free energy landscape

Consider a flexible polymer chain. We start by assuming the free energy landscape for the crossing of the barrier. Consider the chain is affected by a space-fixed potential along the x axis, see Fig. 2,

$$U(x) = -\frac{\omega_B^2}{2}x^2 + \frac{\omega_B^2}{4\xi^2}x^4. \tag{1}$$

The potential has two minima at $x=\pm\xi$ separated by a barrier centered at $x=0$. The barrier has a height of $U_B=U(0)-U(\pm\xi)=\omega_B^2\xi^2/4$ and a width of 2ξ. The curvature of the potential at the maximum is ω_B^2 and at the minima it is $\omega_0^2=2\omega_B^2$. Initially, the chain is trapped in one of the minima (cis) where its free energy per segment is $U(-\xi)=-\omega_B^2\xi^2/4$. It can undergo free motion along y and z-axes. So the initial state of the polymer has a free energy $F(-\xi)=-\omega_B^2\xi^2N_T/4$, where N_T is the total number of segments; see Fig. 3. In the nanofluidic device experiments [7] this can be identified with the DNA in the portion inside the thick region of the channel. Here the polymer can form spherical equilibrium shapes, because the channel thickness is larger than the radius of gyration. In crossing over to the trans side, the long chain molecule pass through a region in space where the free energy per segment is higher, thus effectively presenting a barrier for the motion of the molecule. This corresponds to the thin region where the spherical equilibrium shape cannot be sustained. The molecule gets squeezed in the thin region and the equilibrium structure is deformed. This conformation change costs entropic free energy.

The free energy change in such a situation can be analyzed by the method of scaling [22]. Consider a capillary (or a slit) of diameter (or thickness) $D \ll R$, where $R \sim lN_T^\nu$ is the chain size (l is the Kuhn length; $\nu=3/5$). On length scales less than D, a chain located in the capillary (or slit) is insensitive to the imposed constraint. The maximum length of the unperturbed section of the chain is $(D/l)^{1/\nu}$. This section of polymer segments is called a *blob*. For the estimation of the free energy change, ΔF, associated with the capillary (slit), note that k_BT (k_B is Boltzmann constant and T the temperature) is the only quantity in the problem having the dimension of energy. The polymer is characterized by the only length scale lN_T^ν, so the quantity D can enter all expressions only in the combination $D/(lN_T^\nu)$. The free energy ΔF takes the form

$$\Delta F \sim T\varphi(D/lN_T^\nu), \tag{2}$$

where $\varphi(x)$ is so far an unknown function of the dimensionless argument $x=D/(lN_T^\nu)$. The form of the function $\varphi(x)$ is difficult to derive explicitly, but its asymptotic behavior for the strongly compressed chain ($x \ll 1$) can be established easily. Because of the thermodynamic additivity condition, a macromolecule placed in a narrow slit breaks into many independent parts or blobs. Therefore, $\Delta F \sim N_T$. Hence, $\varphi(x) \sim (x)^{-1/\nu}$, and

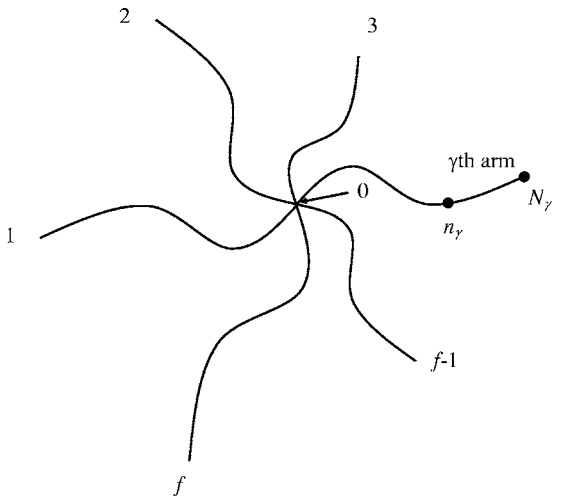

FIG. 4. Schematic illustration of an f-arm star chain. The arm segments are numbered from the center of the star to the end of the chain.

$$\Delta F \sim T N_T (D/l)^{-1/\nu}. \tag{3}$$

The free energy per blob is approximately equal to $k_B T$. This helps to relate the parameters of the potential given by Eq. (1). When a segment is in the barrier region the change in its potential is $U(\pm\xi)-U(0)=\omega_B^2\xi^2/4$. Hence we can now relate the parameters in the model potential with the parameters of the barrier in the experimental situations: $\omega_B^2\xi^2/4 \approx T(D/l)^{-1/\nu}$.

B. The polymer: A star chain

Consider an f-arm star chain with the γth arm composed of N_γ segments. The segments are numbered from the center of the star, $n_\gamma=0$, to the free end of the arm, $n_\gamma=N_\gamma$; see Fig. 4. The total number of beads in the star chain is N_T i.e., $\Sigma_\gamma N_\gamma = N_T$. When there is no potential acting, the star chain exhibits diffusive motion. We first look into this case. Let $\mathbf{r}_\gamma(n_\gamma,t)$ be the spatial position of the n_γ-th segment at time t in three dimensions (3D). The motion of the polymer segments in all the three directions is the same. Hence, it is sufficient to model the chain along any of the axes; we choose to do so along x direction. The dynamics of the star chain can be easily modeled if the molecule is treated as a collection of long chains which are connected at one end but the other end is free. In this case, the continuous form of Rouse-Ham equation [19,20] can be used for modeling the star,

$$\zeta \frac{\partial x_\gamma(n_\gamma,t)}{\partial t} = \kappa \frac{\partial^2 x_\gamma(n_\gamma,t)}{\partial n_\gamma^2} + F(n_\gamma,t), \quad \gamma = 1,\ldots,f. \tag{4}$$

Here, ζ is the segmental friction coefficient of the Rouse segments, $\kappa(=3k_BT/l^2)$ accounts for the increase in free energy on stretching the chain and F is a random force, characterized by moments $\langle F(n_\gamma,t)\rangle=0$ and $\langle F(n_\gamma,t)F(n'_\gamma,t')\rangle = 2\zeta k_B T\delta(n_\gamma-n'_\gamma)\delta(t-t')$. The boundary conditions are

$$\frac{\partial x_\gamma(n_\gamma,t)}{\partial n_\gamma} = 0 \quad \text{at } n_\gamma = N_\gamma, \quad \gamma = 1,\ldots,f \tag{5}$$

at the free end and

$$\sum_{\gamma=1}^{f} \left.\frac{\partial x_\gamma(n_\gamma)}{\partial n_\gamma}\right|_{n_\gamma=0} = 0, \tag{6}$$

$$x_\alpha = x_\beta \quad \text{at } n_\alpha = n_\beta = 0 \quad \text{for } \alpha,\beta = 1,\ldots,f \tag{7}$$

at the center of the star chain.

The eigenfunctions for $x_\gamma(n_\gamma,t)$ satisfying Eqs. (4) and (7) are classified into two groups: $S_{\gamma,k}$ and $C_{\gamma,p}$, *having* and *not having* a node at the connected end ($n_\gamma=0$), respectively. Using these functions we can expand $x_\gamma(n_\gamma,t)$ as

$$\{x_\gamma(n_\gamma,t)\} = X_0(t)\{1\} + \sum_p X_p(t)\{C_{\gamma,p}(n_\gamma)\} + \sum_k \{Y_{\gamma,2k-1}(t)S_{\gamma,2k-1}(n_\gamma)\}, \tag{8}$$

$$C_{\gamma,p} = \frac{\cos\lambda_p(N_\gamma - n_\gamma)}{\cos\lambda_p N_\gamma}, \quad S_{\gamma,2k-1} = \sin\left(\frac{2k-1}{2N_\gamma}\pi n_\gamma\right). \tag{9}$$

Here $\{\cdots\}$ means an array of f quantities (with $\gamma=1,\ldots,f$); X and Y are the amplitude vectors of eigenfunctions $C_{\gamma,p}$ and $S_{\gamma,k}$, respectively. λ_p is the eigenvalue for $C_{\gamma,p}$ determined by

$$\sum_{\gamma=1}^{f} \tan\lambda_p N_\gamma = 0, \quad p = 1,2,\ldots. \tag{10}$$

The boundary condition, Eq. (6), implies that the functions $S_{\gamma,k}$ (and hence $Y_{\gamma,2k-1}$) are not completely independent of each other. Thus we need to specify independent eigenfunctions according to the two cases described below, so that the expansion given in Eq. (8) is a well defined expansion.

Case 1: If $j(\geq 2)$ integers $k_{\gamma_1}, k_{\gamma_2}, \ldots, k_{\gamma_j}$ satisfying

$$\frac{2k_{\gamma_1}-1}{N_{\gamma_1}} = \frac{2k_{\gamma_2}-1}{N_{\gamma_2}} = \cdots = \frac{2k_{\gamma_j}-1}{N_{\gamma_j}} = \frac{2k^*-1}{N^*} \tag{11}$$

exists, the $\gamma_1,\gamma_2,\ldots,\gamma_j$th arms, have the degenerate eigenfunctions $S_{\gamma_j,2k_{\gamma_j}-1}=\sin[(2k^*-1)\pi n_\gamma/2N^*]$ with the same eigenvalue $(2k^*-1)\pi/2N^*$, and the amplitude factors should satisfy

$$\sum_{i=1}^{j} Y_{\gamma_i,2k_{\gamma_i}-1} = 0. \tag{12}$$

For this case we have $j-1$ independent eigenfunctions.

Case 2: If no integers k_α satisfy

$$\frac{2k_\gamma-1}{N_\gamma} = \frac{2k_\alpha-1}{N_\alpha}, \quad \alpha = 1,\ldots,\gamma-1,\gamma+1,\ldots,f \tag{13}$$

for a given integer k_γ (for the γth arm), $S_{\gamma,2k_\gamma-1}$ is not a proper eigenfunction, and $Y_{\gamma,2k_\gamma-1}=0$.

For the chain at equilibrium at $t=0$, the average time evolution of $Y_{\gamma,2k_\gamma-1}$ belonging to the case 1 is characterized by the second moment

$$\langle Y_{\gamma,2k_\gamma-1}(t)Y_{\alpha,2k_\alpha-1}(0)\rangle = \langle Y_{\gamma,2k_\gamma-1}Y_{\alpha,2k_\alpha-1}\rangle_{eq} \times \exp\left[-\frac{\kappa\pi^2 t}{\zeta}\left(\frac{2k_\beta-1}{2N_\beta}\right)^2\right], \tag{14}$$

where $\langle\cdots\rangle_{eq}$ denotes the average at equilibrium. The second moment of X_p is similarly characterized as

$$\langle X_p(t)X_q(0)\rangle = \langle X_pX_q\rangle_{eq}\exp\left(-\frac{\kappa\lambda_p^2 t}{\zeta}\right). \tag{15}$$

The averages at equilibrium are evaluated by

$$\langle ZZ'\rangle = \frac{\int_{-\infty}^{\infty}\{dZ''\}ZZ'\psi(\{Z''\})}{\int_{-\infty}^{\infty}\{dZ''\}\psi(\{Z''\})}, \tag{16}$$

where Z, Z', and Z'' indicate amplitude vectors X and Y, and the equilibrium distribution function ψ for these vectors is given by

$$\psi \propto \exp\left[-\frac{\kappa}{2kT}\sum_{\gamma=1}^{f}\int_0^{N_\gamma}\left(\frac{\partial x_\gamma}{\partial n_\gamma}\right)^2 dn_\gamma\right]. \tag{17}$$

III. THE RATE CALCULATION

A. Multidimensional Kramers' rate theory

We are interested in finding out what is the rate or the inverse mean time of the thermally activated crossing of the whole chain from one well to the other. To simplify the problem, we confine ourselves to the overdamped case where the crossing dynamics is much slower than the internal chain relaxation. In this case a multidimensional Kramers' theory [16] is directly applicable. For the interaction between the beads only the nearest neighbor coupling characterized by the potential $V(\Delta\mathbf{r})=V(|\mathbf{r}(n+1)-\mathbf{r}(n)|)$ is considered. We neglect other interbead interactions that give rise to the excluded volume effect and bending stiffness. In dilute solutions, the Rouse-Ham model [20,24], which is a simple bead spring model, gives a satisfactory description of the conformation and dynamics of a real polymer. Strictly speaking, the segmental "spring" of a real polymer in presence of a rapidly varying potential is no longer linear, as assumed in Rouse-Ham model. However, if the barrier height is less than k_BT per segment [23], i.e., $\omega_B^2\xi^2 < k_BT$, the nonlinear terms in $V(\Delta\mathbf{r})$ may be safely neglected.

The total energy of the chain in presence of the potential U is

$$\Phi[\mathbf{r}_\gamma(n_\gamma)] = \sum_{n_\gamma} U[\mathbf{r}_\gamma(n_\gamma)] + \sum_{n_\gamma}\frac{3k_BT}{2l^2}|\mathbf{r}_\gamma(n_\gamma+1)-\mathbf{r}_\gamma(n_\gamma)|^2. \tag{18}$$

The summation is over all polymer segments of the star chain. The focus is on the overdamped limit where the bead's momentum relaxation has already occurred. In this limit, the escape process can be regarded as a Brownian motion occurring in the $3N$-dimensional configuration space of the chain, where the above energy function, Eq. (18), is defined. Noting that the energy function does not involve coupling between different Cartesian coordinates, the problem can be further reduced by considering the dynamics only along the x direction. Note that the potential is varying only along this axis, along other axes the potential is invariant; see Fig. 2. The polymer dynamics is then governed by the energy function

$$\Phi[x_\gamma(n_\gamma)] = \sum_{n_\gamma} U[x_\gamma(n_\gamma)] + \sum_{n_\gamma}\frac{3k_BT}{2l^2}|x_\gamma(n_\gamma+1)-x_\gamma(n_\gamma)|^2. \tag{19}$$

The probability per unit volume of the chain to have configuration $x_\gamma(n_\gamma)$ at time $t, P[x_\gamma(n_\gamma),t]$ satisfies the Fokker-Planck equation

$$\frac{\partial P}{\partial t} = D\sum_m \frac{\partial}{\partial x_m}\left[\frac{\partial}{\partial x_m}+\beta\frac{\partial}{\partial x_m}\Phi\right]P. \tag{20}$$

The summation is over all segments of the star chain. Here, D is the segmental diffusion coefficient and $\beta=(k_BT)^{-1}$. In y and z directions the star chain simply shows the free space Rouse-Ham [19,20] chain dynamics.

The configuration space of the star polymer $\{x_\gamma(n_\gamma)\}$ contains two stable points that correspond to the chains localized at $x=+\xi$ or $x=-\xi$. These two states, which will be denoted by $\{\bar{x}\}_+$ and $\{\bar{x}\}_-$, respectively, are separated by a higher-energy region, or barrier, in the $\{x_\gamma(n_\gamma)\}$ space. The problem is to find the rate at which the star chain starts from its initial confinement around $\{\bar{x}\}_-$ and escapes over the barrier to reach the well around $\{\bar{x}\}_+$. The activation energy of this process is the lowest threshold energy in all the paths connecting the states $\{\bar{x}\}_-$ and $\{\bar{x}\}_+$. Geometrically, it is determined by the path crossing the saddle point $\{\bar{x}\}_B$ in the configuration space, which is a stationary point with respect to a variation satisfying

$$\left.\frac{\delta\Phi}{\delta x_\gamma(n_\gamma)}\right|_{\{\bar{x}\}_B} = 0 \tag{21}$$

and involving only one unstable mode along which the "reaction flux" runs from $\{\bar{x}\}_-$ to $\{\bar{x}\}_+$. This "transition state" $\{\bar{x}\}_B$ corresponds to either a localized configuration [23] of $\{x_\gamma(n_\gamma)\}$ around $x=0$, or a kink configuration [21] representing a stretched chain around $x=0$, depending on the star chain and the potential parameters.

We denote the activation energy as $\Delta\Phi=\Phi[\{\bar{x}\}_B]-\Phi[\{\bar{x}\}_-]$. If $\Delta\Phi \gg k_BT$, the crossing time is greater than any internal chain relaxation time, and it can be calculated from an approximate, quasi-stationary solution to Eq. (20). The rate is obtained by dividing the reaction flux j across the saddle point $\{\bar{x}\}_B$ by the total probability population confined in the well at $\{\bar{x}\}_-$. The resulting rate $\mathcal{R}$ is

$$\mathcal{R} = \frac{\omega_B}{2\pi\zeta}\frac{Z_B}{Z_0}\sqrt{2\pi k_B T}e^{-\beta\Delta\Phi}, \tag{22}$$

where Z_0 and Z_B are the partition functions associated with the fluctuation of the system near the initial stable point $\{\bar{x}\}_-$ and the saddle point $\{\bar{x}\}_B$, respectively,

$$Z_0 = \int_{well} d^N\{x(n_\gamma)\}e^{-\beta[\Phi(\{x_\gamma\})-\Phi(\{\bar{x}\}_-)]}, \tag{23}$$

$$Z_B = \int_{barrier} d^{N-1}\{x(n_\gamma)\}e^{-\beta[\Phi(\{x_\gamma\})-\Phi(\{\bar{x}\}_B)]}. \tag{24}$$

The integration in Z_B is over the hypersurface which contains the saddle point but is normal to the unstable mode.

The above rate formalism can be applied to our problem if we identify a well defined transition state of the chain represented by a localized saddle point in the configuration space. This can be seen by noting that Eq. (22) gives the rate in terms of only the local properties of the saddle and the metastable points, without showing dependence on the details of the activation processes. One example of such dependence is when the chain contour length is much larger than the width of the barrier so that the chain translocation from one well to the other occurs via movement of a stretched portion of the chain, or a kink along the chain [14].

B. The star chain in double well

Consider the space fixed quartic potential $U(x)$ (see Fig. 2), where the barrier width is larger than the length of each of the arms of the chain. In this potential the variational relationship equation (21) has three solutions consistent with the chain boundary conditions,

$$\{\bar{x}_\gamma(n_\gamma)\} \equiv 0, \pm\xi. \tag{25}$$

Among these, the solutions corresponding to the chains confined in either well, $\{\bar{x}_\gamma(n_\gamma)\} \equiv \pm\xi$, are stable. Assume that the chain is initially confined in the left well near $x=-\xi$, so that the metastable configuration is denoted by $\bar{x}_0=\{\bar{x}\}_- \equiv -\xi$. The subscript 0 indicates that this is the configuration at time $t=0$. The homogeneous configuration $\bar{x}_\gamma(n_\gamma)\equiv 0$ is the only saddle point (in the $\{\bar{x}_\gamma(n_\gamma)\}$ space) bridging the two stable states $\{\bar{x}_\gamma(n_\gamma)\} \equiv \pm\xi$. We denote such a transition state as $\{\bar{x}\}_B$.

To assess the effects of the fluctuation and the saddle point structure of the chain energy functional we investigate the eigenvalue spectrum of the operator of the second order expansion of Φ at the stationary points. This operator is defined by the expansion

$$\Phi[\bar{x}+\delta x] = \Phi[\bar{x}] + \frac{1}{2}\int dn\ \delta x(n)\mathbf{\Phi}\delta x(n) + O[(\delta x)^4], \tag{26}$$

where the integration is over all chain segments [25]. The differential operator corresponds to

$$\mathbf{\Phi} \Leftrightarrow U''[\{\bar{x}_\gamma(n_\gamma)\}] - \kappa\frac{d^2}{dn^2}. \tag{27}$$

The operator $-\kappa(d^2/dn^2)$ has nondegenerate eigenfunctions $C_{\gamma,p}$ with the eigenvalue spectrum $\kappa\lambda_p^2$, where $p=0,1,\ldots$ and $\gamma=1,2,\ldots,f$, see Eq. (9). These are associated with the Rouse modes *not having* a node at the connected end $n_\gamma=0$. The eigenvalues associated with the Rouse modes *having* a node at the connected end can be found by the two cases discussed in the last section. For case 1 the operator $-\kappa(d^2/dn^2)$ have $j-1$ degenerate eigenfunctions $S_{\gamma_j,2k_{\gamma j}-1} = \sin[(2k^*-1)\pi n_\gamma/2N^*]$ with the same eigenvalue $\kappa(2k^*-1)^2\pi^2/4N^{*2}$ for j integers satisfying Eq. (11). For case 2 there are no proper eigenfunctions having a node at the connected end. Note that the total number of eigenmodes is equal to the total number of Rouse segments in the star chain.

The curvature of the potential at the minima is $U''(-\xi) = 2\omega_B^2 = \omega_0^2$. The eigenvalues of $\mathbf{\Phi}$ for the chain in the metastable well $\{\bar{x}\}_-$ are obtained by shifting the eigenvalues for the star chain in free space by ω_0^2. Thus the eigenvalues are $\lambda_p^0 = \omega_0^2 + \kappa\lambda_p^2$, where $p=0,1,\ldots$ and $\lambda_{k^*}^0 = \omega_0^2 + \kappa(2k^*-1)^2\pi^2/4N^{*2}$ for all integers satisfying Eq. (11). Note that for $\{\bar{x}\}_-$ all eigenvalues are positive, confirming that these are solutions of Eq. (21) corresponding to stable configurations.

Consider the saddle point $\{\bar{x}\}_B \equiv 0$. The curvature of the potential at the maximum is $U''(0) = -\omega_B^2$. The eigenvalues of $\mathbf{\Phi}$ for this state are obtained by shifting the eigenvalues for the free star chain by $-\omega_B^2$. They are $\lambda_p^B = -\omega_B^2 + \kappa\lambda_p^2$, where $p=0,1,\ldots$ and $\lambda_{k^*}^B = -\omega_B^2 + \kappa(2k^*-1)^2\pi^2/4N^{*2}$ for all integers satisfying Eq. (11). In this state the smallest eigenvalue is $-\omega_B^2$, which is negative. The next eigenvalue, associated with the first Rouse mode $C_{\gamma,1}$ and/or $S_{\gamma,1}$ is positive as long as $\omega_B^2 < \kappa\lambda_1^2$ and/or $\omega_B^2 < \kappa\pi^2/N_\gamma^2$, for all N_γ. Thus, as long as the conditions $\omega_B^2 < \kappa\lambda_1^2$ and/or $\omega_B^2 < \kappa\pi^2/N_\gamma^2$ are satisfied, the state $\{\bar{x}\}_B \equiv 0$ is indeed the saddle point with only one unstable eigenmode $C_{\gamma,0} \equiv 1$. This constitutes the transition state of the chain bridging the two stable configurations. As the configuration $\{\bar{x}\}_B \equiv 0$ corresponds to a compact chain conformation at the barrier top and the single unstable mode $C_{\gamma,0}$ represents uniform translation in the x direction of the whole chain, we conclude that the star chain crosses the barrier in a compact form.

In this compact-state barrier crossing regime, let us calculate the rate $\mathcal{R}$. The net barrier height $\Delta\Phi$ is the difference between the energies of the two stationary states $\{\bar{x}\}_B$ and $\{\bar{x}\}_-$:

$$\Delta\Phi = \Phi[\{\bar{x}\}_B] - \Phi[\{\bar{x}\}_-] = \sum_\gamma N_\gamma U_B = N_T U_B. \tag{28}$$

The partition functions accounting for the free energies of fluctuation at the well and the saddle state are calculated from the functional integrations

$$Z_0 = \int_{well} \mathcal{D}[\delta x(n)]e^{-\beta\{\Phi[\bar{x}_0+\delta x]-\Phi[\bar{x}_0]\}}, \tag{29}$$

$$Z_B = \int_{saddle} \mathcal{D}[\delta x(n)] e^{-\beta\{\Phi[\bar{x}_B+\delta x]-\Phi[\bar{x}_B]\}}. \tag{30}$$

The integration Z_B is over all modes except the unstable mode which leads to the barrier crossing. For integrating over fluctuation $\delta x(n)$ we express the fluctuations of the chains at the extrema in terms of the eigenfunctions $C_{\gamma,p}$ and $S_{\gamma,k}$ of the operator $\mathbf{\Phi}$:

$$\delta x(n) = \sum_{\gamma,p} X_{\gamma,p} C_{\gamma,p} + \sum_{\gamma,k} Y_{\gamma,2k-1} S_{\gamma,2k-1}. \tag{31}$$

Substituting this in Eqs. (29) and (30) and performing the integrations within the harmonic approximation for the variation in Φ leads to the partition functions

$$Z_0 = (\sqrt{2\pi k_B T})^{N_T} (\lambda_0^0 \ldots)^{-1/2} \{(\lambda_{k^*}^0)^{j-1} \ldots\}^{-1/2}, \tag{32}$$

$$Z_B = (\sqrt{2\pi k_B T})^{N_T-1} (\lambda_1^B \ldots)^{-1/2} \{(\lambda_{k^*}^B)^{j-1} \ldots\}^{-1/2}. \tag{33}$$

Finally, from Eq. (22) we obtain

$$\mathcal{R} = \frac{\omega_B}{2\pi\zeta} \frac{(\lambda_0^0 \ldots)^{1/2}}{(\lambda_1^B \ldots)^{1/2}} \frac{\{(\lambda_{k^*}^0)^{j-1} \ldots\}^{1/2}}{\{(\lambda_{k^*}^B)^{j-1} \ldots\}^{1/2}} e^{-\beta N_T U_B} \tag{34}$$

$$= \frac{\omega_B \omega_0}{2\pi\zeta} \left[\prod_{p(\neq 0)} \frac{(\omega_0^2 + \kappa\lambda_p^2)^{1/2}}{(-\omega_B^2 + \kappa\lambda_p^2)^{1/2}} \right] \times \left[\prod_{k^*} \frac{(\omega_0^2 + \kappa(2k^*-1)^2\pi^2/4N^{*2})^{(j-1)/2}}{(-\omega_B^2 + \kappa(2k^*-1)^2\pi^2/4N^{*2})^{(j-1)/2}} \right] e^{-\beta N_T U_B} \tag{35}$$

for $-\omega_B^2 + \kappa\lambda_p^2 > 0$ and $-\omega_B^2 + \kappa(2k^*-1)^2\pi^2/4N^{*2} > 0$.

Equation (35) has several hidden features which demands attention. When there are arms of equal length the Rouse modes of these arms not having a node at the center are the same. They are no longer independent. However, these arms also give rise to modes having a node at the center, which are degenerate. Thus, whenever there are modes with a node at the center of the star chain there is also a linear dependence of modes not having a node at the center. These issues are illustrated in Secs. III C and III D.

As the flexibility of the chains decreases or when the polymer is in a poor solvent, the polymer behaves like a compact globule. In this strong coupling limit $l \to 0$ (or $\kappa \to \infty$) the rate becomes that for a single particle in the double well

$$\mathcal{R}(l \to 0) \to \frac{\omega_B \omega_0}{2\pi\zeta} e^{-\beta N_T U_B} \equiv \mathcal{R}_0. \tag{36}$$

$\mathcal{R}_0$ is the rate expected when the star chain acts like a single compact globule. As the chain becomes larger the rate increases. For all range of parameters satisfying the conditions $-\omega_B^2 + \kappa\lambda_p^2 > 0$ and $-\omega_B^2 + \kappa(2k^*-1)^2\pi^2/4N^{*2} > 0$, the activation energy itself remains constant. The effect of flexibility is wholly contained in the *prefactor* of the rate, Eq. (35), representing the effect of the fluctuations of star in the well and on top of the barrier. For a fixed κ, the rate $\mathcal{R}$ *compared to* its strong coupling limit, increases on increasing the length of any of the arms of the star chain by a factor of

$$\frac{\mathcal{R}}{\mathcal{R}_0} = \left[\prod_{p(\neq 0)} \frac{(\omega_0^2 + \kappa\lambda_p^2)^{1/2}}{(-\omega_B^2 + \kappa\lambda_p^2)^{1/2}} \right] \times \left[\prod_{k^*} \frac{(\omega_0^2 + \kappa(2k^*-1)^2\pi^2/4N^{*2})^{(j-1)/2}}{(-\omega_B^2 + \kappa(2k^*-1)^2\pi^2/4N^{*2})^{(j-1)/2}} \right]. \tag{37}$$

Equation (37) also shows that for a given total molecular weight of a polymer the rate prefactor can differ widely depending upon the architecture of the polymer.

In all the above analysis the parameter range considered is $-\omega_B^2 + \kappa\lambda_p^2 > 0$ and $-\omega_B^2 + \kappa(2k^*-1)^2\pi^2/4N^{*2} > 0$. When $-\omega_B^2 + \kappa\lambda_p^2 \to 0$ and/or $-\omega_B^2 + \kappa(2k^*-1)^2\pi^2/4N^{*2} \to 0$ the rate $\mathcal{R}$ diverges. This happens when the eigenvalue of the internal Rouse modes of the star polymer at the top of the barrier matches with the curvature of the external potential. The polymer undergoes a coil-to-stretch transition [26]. As the motional modes of the polymer extend over different arms of the molecule and the multiplicity of arms leads to the degeneracy of the modes, there emerges multiple pathways for the barrier crossing. Each singularity in the rate expression points to an opening of a pathway to lower the free energy which effectively increases the rate of the barrier crossing. However, when the barrier curvature is small on the microscopic scale and the barrier width is large compared to the size of the polymer, the escape process is dominated by the activation of the entire chain over the barrier.

For a general arm-length distribution, it is difficult to solve Eq. (10) analytically and find an explicit expression for λ_p. It is also difficult to find appropriate k values satisfying Eq. (11) and giving nonzero $Y_{\gamma,2k-1}$ factors. We thus analyze the dynamics of model f-arm stars with simple structures: star chains with all arms having equal lengths and star chains with a distribution of arms having lengths N and $2N$. Using these results we find the barrier crossing rates for the star chains. For a star chain, other than the two classes, the difficulty in solving Eq. (10) analytically in closed form leaves us only the method of numerically finding the rates of barrier crossing. However, the method is clearly outlined in Sec. III A and Eqs. (32)–(35).

C. Star chain with equal arms

Consider an f-arm star chain composed of arms of *equal* lengths $N_1 = N_2 = \cdots = N_f = N$. When there is no external potential acting on the chain the star polymer exhibits diffusive dynamics. The position vector of the chain segments can then be expanded in terms of modes as shown in Eq. (8). For the eigenmodes not having a node at the connected end, $C_{\gamma,p}$, the eigenvalue equation (10) is simplified to

$$\tan \lambda_p N = 0, \quad \lambda_p = p\pi/N, \quad p = 1,2,\ldots \tag{38}$$

so that $C_{\gamma,p} = \cos(p\pi n_\gamma/N)$. Note that $C_{\gamma,p}$ are nondegenerate eigenfunctions. The eigenmodes having a node at the connected end $S_{\gamma,2k-1} = \sin([(2k-1)/2N]\pi n_\gamma)$ are degenerate for the arms, leading to the relation

$$\sum_{k=1}^{f} Y_{\gamma,2k-1} = 0 \quad \text{for } k = 1,2,\ldots. \tag{39}$$

We have $f-1$ independent [20] eigenfunctions $S_{\gamma,2k-1}$.

Consider the star is effected by the space fixed quartic potential in Eq. (1). The width of the barrier is assumed to be larger than the length of each arm of the star chain as shown in Fig. 3. For the chain trapped in the metastable well $\{\bar{x}\}_-$ the eigenvalue spectrum of the operator $\mathbf{\Phi}$, defined by Eq. (27), is $\omega_0^2+\kappa\pi^2p^2/N^2$ and $\omega_0^2+\kappa(2k-1)^2\pi^2/4N^2$, with $p=0,1,\ldots$ and $k=1,2,\ldots$, respectively. For the chain at the saddle point $\{\bar{x}\}_B$ the eigenvalue spectrum of $\mathbf{\Phi}$ is $-\omega_B^2+\kappa\pi^2p^2/N^2$ and $-\omega_B^2+\kappa(2k-1)^2\pi^2/4N^2$ with the same p and k, respectively, as in the potential well.

The net barrier height $\Delta\Phi$ is the difference between the energies of the two stationary states $\{\bar{x}\}_B$ and $\{\bar{x}\}_-$:

$$\Delta\Phi = \Phi[\{\bar{x}\}_B] - \Phi[\{\bar{x}\}_-] = fNU_B = N_TU_B. \tag{40}$$

The partition functions Z_0 and Z_B accounting for the free energies of fluctuations at the well and the saddle state, respectively, are calculated from the functional integrals (29) and (30). The integrations over fluctuations $\delta x(n)$ can be done by expressing the fluctuations of the chains in terms of the eigenfunctions $C_{\gamma,p}$ and $S_{\gamma,2k-1}$ of the operator $\mathbf{\Phi}$. On performing the integrations within the harmonic approximation for the variations in Φ, the partition functions are

$$Z_0 = (\sqrt{2\pi k_BT})^{fN}\left[\prod_p (\omega_0^2+\kappa\pi^2p^2/N^2)^{1/2}\right] \times\left[\prod_k (\omega_0^2+\kappa(2k-1)^2\pi^2/4N^2)^{(f-1)/2}\right], \tag{41}$$

$$Z_B = (\sqrt{2\pi k_BT})^{fN-1}\left[\prod_p (-\omega_B^2+\kappa\pi^2p^2/N^2)^{1/2}\right] \times\left[\prod_k (-\omega_B^2+\kappa(2k-1)^2\pi^2/4N^2)^{(f-1)/2}\right]. \tag{42}$$

Substituting these partition functions into Eq. (22), we obtain

$$\mathcal{R} = \frac{\omega_B\omega_0}{2\pi\zeta}\left[\prod_p \frac{(\omega_0^2+\kappa\pi^2p^2/N^2)^{1/2}}{(-\omega_B^2+\kappa\pi^2p^2/N^2)^{1/2}}\right] \times\left[\prod_k \frac{(\omega_0^2+\kappa(2k-1)^2\pi^2/4N^2)^{(f-1)/2}}{(-\omega_B^2+\kappa(2k-1)^2\pi^2/4N^2)^{(f-1)/2}}\right] e^{-\beta fNU_B}, \tag{43}$$

$$\approx \frac{\omega_B\omega_0}{2\pi\zeta}\left(\frac{\omega_B^2}{\omega_0^2}\right)^{1/4}\left(\frac{\sinh(N\sqrt{\omega_0^2/\kappa})}{\sin(N\sqrt{\omega_B^2/\kappa})}\right)^{1/2} \times\left(\frac{\cosh(N\sqrt{\omega_0^2/\kappa})}{\cos(N\sqrt{\omega_B^2/\kappa})}\right)^{(f-1)/2} e^{-\beta N_TU_B}. \tag{44}$$

The last approximation holds for all $N\gg 1$.

The rate can also be expressed in terms of the radius of gyration. For an f-arm star polymer of equal arm lengths the radius of gyration is [27]

$$\mathbf{r}_g^2 = Nl^2\left(\frac{1}{2}-\frac{1}{3f}\right). \tag{45}$$

Using this in Eq. (44),

$$\mathcal{R} \approx \frac{\omega_B\omega_0}{2\pi\zeta}\left(\frac{\omega_B^2}{\omega_0^2}\right)^{1/4}\left(\frac{\sinh(z_0)}{\sin(z_B)}\right)^{1/2}\left(\frac{\cosh(z_0)}{\cos(z_B)}\right)^{(f-1)/2} e^{-\beta N_TU_B} \tag{46}$$

$$= \frac{\omega_B\omega_0}{2\pi\zeta}\left(\frac{\omega_B^2}{\omega_0^2}\right)^{1/4}\left(\frac{e^{z_0}-e^{-z_0}}{2\sin(z_B)}\right)^{1/2}\left(\frac{e^{z_0}+e^{-z_0}}{2\cos(z_B)}\right)^{(f-1)/2} e^{-\beta N_TU_B}, \tag{47}$$

where $z_0=(\mathbf{r}_g^2\sqrt{\omega_0^2/\kappa}/l^2(\frac{1}{2}-1/3f))$ and $z_B=(\mathbf{r}_g^2\sqrt{\omega_B^2/\kappa}/l^2(\frac{1}{2}-1/3f))$.

As the flexibility of the star arms decreases the strong coupling limit is reached. In this limit the barrier crossing rate is given by Eq. (36).

D. Star chain with bimodal arm length distribution

We consider an ensemble of long and short linear chains of lengths $2N$ and N, respectively. Using these as *precursors*, one can make f-arm star chains with a distribution of short and long arms. In the following star chains composed of α short and $f-\alpha$ long arms is considered. For this polymer the eigenvalue equation for $C_{\gamma,p}$ reduces to

$$\alpha\tan\lambda_pN + (f-\alpha)\tan 2\lambda_pN = 0 \tag{48}$$

which in turn leads to three sequences of eigenvalues [20],

$$\lambda_p = p\pi/N, \quad \lambda_p' = (p-1+\chi_\alpha)\pi/N \quad \text{and} \tag{49}$$

$$\lambda_p'' = (p-\chi_\alpha)\pi/N, \quad p = 1,2,\ldots$$

with

$$\chi_\alpha = (1/\pi)\cos^{-1}\sqrt{\alpha/2f} \quad (0<\chi_\alpha<1/2). \tag{50}$$

For the eigenmodes $S_{\gamma,2k-1}$ note that the integers satisfying Eq. (11) are found only for arms of the same length, N or $2N$.

The eigenvalues of the operator $\mathbf{\Phi}$ for the star chain inside the metastable well $\{\bar{x}\}_-$ thus leads to five sequences. The eigenvalues due to the modes *not having* a node at the connected end are $\omega_0^2+\kappa\pi^2p^2/N^2$, $\omega_0^2+\kappa\pi^2(p-1+\chi_\alpha)^2/N^2$ and $\omega_0^2+\kappa\pi^2(p-\chi_\alpha)^2/N^2$, with, $p=1,2,\ldots$. The eigenvalues due to the modes *having* a node at the connected end are $\omega_0^2+\kappa(2k-1)^2\pi^2/4N^2$, with $k=1,2,\ldots$ and $\omega_0^2+\kappa(2k'-1)^2\pi^2/16N^2$, with $k'=1,2,\ldots$. Similarly, for the chain at the saddle point $\{\bar{x}\}_B$, the operator $\mathbf{\Phi}$ has five sequences of eigenvalues. The eigenvalues due to the modes *not having* a node at the connected end are $-\omega_B^2+\kappa\pi^2p^2/N^2$, $-\omega_B^2+\kappa\pi^2(p-1+\chi_\alpha)^2/N^2$ and $-\omega_B^2+\kappa\pi^2(p-\chi_\alpha)^2/N^2$, with $p=1,2,\ldots$. The eigenvalues due to the modes *having* a node at the connected end are $-\omega_B^2+\kappa(2k-1)^2\pi^2/4N^2$, with $k=1,2,\ldots$ and $-\omega_B^2+\kappa(2k'-1)^2\pi^2/16N^2$, with $k'=1,2,\ldots$. Substituting these eigenvalues into Eq. (34) we obtain rate of barrier crossing

$$\mathcal{R} = \frac{\omega_B \omega_0}{2\pi\zeta}\left[\prod_p \frac{\left(\omega_0^2 + \frac{\kappa\pi^2}{N^2}p^2\right)^{1/2}}{\left(-\omega_B^2 + \frac{\kappa\pi^2}{N^2}p^2\right)^{1/2}} \times \frac{\left(\omega_0^2 + \frac{\kappa\pi^2}{N^2}(p-1+\chi_\alpha)^2\right)^{1/2}}{\left(-\omega_B^2 + \frac{\kappa\pi^2}{N^2}(p-1+\chi_\alpha)^2\right)^{1/2}} \times \frac{\left(\omega_0^2 + \frac{\kappa\pi^2}{N^2}(p-\chi_\alpha)^2\right)^{1/2}}{\left(-\omega_B^2 + \frac{\kappa\pi^2}{N^2}(p-\chi_\alpha)^2\right)^{1/2}}\right] \times \left[\prod_k \frac{\left(\omega_0^2 + \frac{\kappa\pi^2}{4N^2}(2k-1)^2\right)^{(\alpha-1)/2}}{\left(-\omega_B^2 + \frac{\kappa\pi^2}{4N^2}(2k-1)^2\right)^{(\alpha-1)/2}}\right] \times \left[\prod_{k'} \frac{\left(\omega_0^2 + \frac{\kappa\pi^2}{16N^2}(2k'-1)^2\right)^{(f-\alpha-1)/2}}{\left(-\omega_B^2 + \frac{\kappa\pi^2}{16N^2}(2k'-1)^2\right)^{(f-\alpha-1)/2}}\right] e^{-\beta N_T U_B}. \tag{51}$$

When $N \gg 1$ the rate can be approximated to

$$\mathcal{R} \approx \frac{\omega_B \omega_0}{2\pi\zeta}\left(\frac{\omega_B^2}{\omega_0^2}\right)^{1/4}\left(\frac{\sinh(N\sqrt{\omega_0^2/\kappa})}{\sin(N\sqrt{\omega_B^2/\kappa})}\right)^{1/2} \times \left(\frac{\cos(2\pi\chi_\alpha) - \cosh(2N\sqrt{\omega_0^2/\kappa})}{\cos(2\pi\chi_\alpha) - \cos(2N\sqrt{\omega_B^2/\kappa})}\right)^{1/2} \times \left(\frac{\cosh(N\sqrt{\omega_0^2/\kappa})}{\cos(N\sqrt{\omega_B^2/\kappa})}\right)^{(\alpha-1)/2} \times \left(\frac{\cosh(2N\sqrt{\omega_0^2/\kappa})}{\cos(2N\sqrt{\omega_B^2/\kappa})}\right)^{(f-\alpha-1)/2} e^{-\beta N_T U_B}. \tag{52}$$

In the strong coupling limit the barrier crossing rate for the star with bimodal arm distribution is again given by Eq. (36).

E. The rate: Near exponential dependence on radius of gyration

Quantitatively, the rate of the thermally activated process equations (34)–(37), (43), (44), (51), and (52) derived by multidimensional-Kramers theory are in the form of the celebrated Arrhenius law:

$$\mathcal{R} = \nu_0 e^{-E_a/K_B T}, \tag{53}$$

where E_a is the activation energy and ν_0 the preexponential factor, which can be thought of as (but not identified with; see above) a frequency characteristic of the system. Once the two parameters E_a and ν_0 are deduced all the details of the system can be predicted within the broad validity regime of Kramers theory.

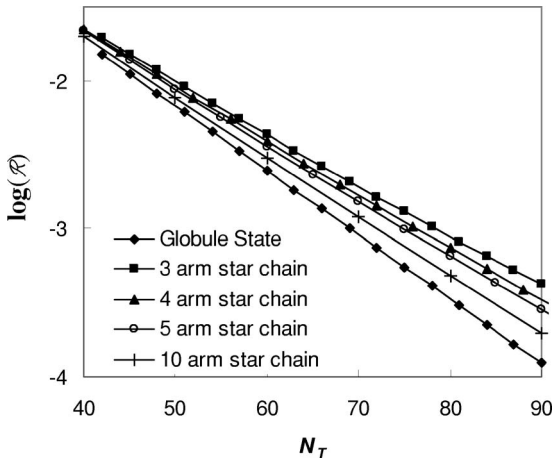

FIG. 5. Plots of the logarithm (with base 10) of the rate of barrier crossing against the total number of segments in the star chain. The stars are considered to have arms of equal lengths. The barrier parameters chosen for the calculation are $\omega_B/\kappa = 1/1200$ and $\xi = 126.5l$.

Of the two parameters determining the rate of the barrier crossing, E_a and ν_0, the activation energy is unquestionably the more important one because it enters Eq. (53) exponentially. In the barrier crossing problem by a star chain the activation energy is proportional to the total number of segments in the star chain. This exponential dependence of the barrier crossing rate for stars having different structures is illustrated in Fig. 5.

Less attention is generally paid to the pre-exponential factor ν_0, primarily because it enters the same equation only linearly. The justification for this uneven balance of attention comes from a vast amount of accumulated data for a wide variety of material systems. However, for the present system the rate prefactor has a significant role in the barrier crossing mechanism. The prefactor holds the collective dynamics of the star chain and can differ widely depending upon the architecture of the stars. Star chains having the same number of total Rouse segments N_T, can have varied structures. For example, a star having six arms each consisting of ten segments and a star having three arms, each having 20 segments, have the same total number of segments $N_T = 60$. However they have different radius of gyration $\mathbf{r}_g$ [27]. The longer arms give rise to extended motional modes. The star moves at random within the well until a large fluctuation propels it out of the well over the energy barrier. Molecules with larger radius of gyration can effect larger fluctuations, thereby increasing its frequency to escape over the barrier. In Tables I and II we list different star polymers while keeping the total number of Rouse segments constant. These molecular structures have a range of radius of gyration. Here again we see that the stars with a larger radius of gyration have higher crossing rates. The effect of the radius of gyration on the rate prefactors is clearly seen in Fig. 6. This plot shows that the rate prefactor depends almost *exponentially* upon the

TABLE I. Comparison of the molecular architectures, radius of gyrations, and reduced barrier crossing rates for multiarm star chains, keeping the total number of segments constant $N_T=60$.

No. of arms (f)	No. of short arms (α)	No. of long arms ($f-\alpha$)	Length of arms/ short arms (N)	Reduced mean square radius of gyration ($r_g^2/N_T l^2$)	Reduced rate ($\mathcal{R}/\mathcal{R}_0$)
3			20	0.778	1.739
4			15	0.625	1.567
5			12	0.520	1.455
6			10	0.444	1.379
10			6	0.280	1.223
3	2	1	15	0.812	1.777
3	1	2	12	0.808	1.773
4	3	1	12	0.664	1.607
4	2	2	10	0.666	1.610
5	4	1	10	0.555	1.491
6	2	4	6	0.472	1.406
7	2	5	5	0.409	1.345
7	4	6	6	0.424	1.358

radius of gyration. However, it is difficult to see this from the analytical expressions, even in the simplest case where all the arms of the chain are of equal length; see Eq. (47).

In experimental situations the exponential dependence of the rate on the radius of gyration can have significant implications. In purification of DNA, the starting material normally contains mixtures of DNA which can have open circular forms or supercoiled structures with varied degrees of writhe and twists [28]. These structures exhibit considerable difference in their dynamics. In the entropic based methods [7] of separation of the DNA, the differences in the dynamics of different structures of the same molecule can be effectively utilized. The separation methods are already an order of magnitude faster than the conventional slab gel pulsed-field gel electrophoresis, with the possibility to achieve better resolution through longer channels. The exponential dependence of the rate on the radius of gyration can thus be used to separate DNA having different kinds of secondary structures.

The rate expressions could also lead to design and fabrication of new separation materials such as hydrogels [6], in which macromolecules could be retarded, trapped and separated. Such materials might also be used as specific biochemical trapping materials for applications in drug delivery and controlled release processes. These may also be used as semi-homogeneous microreactors for applications in organic, bioengineering and combinatorial synthesis. In these applica-

TABLE II. Comparison of the molecular architectures, radius of gyrations, and reduced barrier crossing rates for star chains with $N_T=72$.

No. of arms (f)	No. of short arms (α)	No. of long arms ($f-\alpha$)	Length of arms/ short arms (N)	Reduced mean square radius of gyration ($r_g^2/N_T l^2$)	Reduced rate ($\mathcal{R}/\mathcal{R}_0$)
3			24	0.778	2.203
4			18	0.625	1.902
6			12	0.444	1.588
8			9	0.344	1.431
9			8	0.309	1.379
12			6	0.236	1.277
3	2	1	18	0.812	2.275
4	2	2	12	0.667	1.977
5	4	1	12	0.556	1.772
5	2	3	9	0.554	1.772
5	1	4	8	0.539	1.746
6	4	2	9	0.484	1.651
6	3	3	8	0.481	1.647

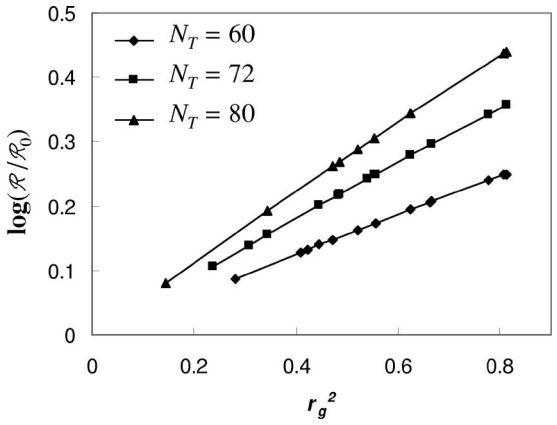

FIG. 6. Plots of the logarithm (with base 10) of the reduced rate of barrier crossing $\mathcal{R}/\mathcal{R}_0$ against the reduced mean square radius of gyration $r_g^2/N_T l^2$; see Tables I and II. The parameters chosen for the barrier are the same as in Fig. 5.

tions, the existence and location of chemical species could be probed by flourescent markers to monitor physiochemical processes in real time.

Finally, we should make a comment on the domain of applicability of the above analysis. The study uses Rouse-Ham model to derive the rate of escape over the barrier. This model accounts for the local interactions along the chain. It neglects hydrodynamic interactions and excluded volume effects which are significant in several systems. Hence the study is applicable to star polymer solutions and other systems where Rouse-Ham model is known to work well. Another domain where the analysis does not hold is when the arms of the star have a contour length much longer than the width of the barrier. In such a situation the barrier crossing occurs via movement of a stretched portion of the chain over the barrier. This process significantly reduces the activation energy and hence increases the rate [14].

IV. CONCLUDING REMARKS

We considered the generalization of the Kramers escape over a barrier problem, to the case of a long chain molecule with a given structure. The escape process consists of the motion of the chain molecule across a region where the free energy per segment is higher, so that it has to cross a barrier. We consider the limit where the width of the barrier is larger compared to the length of each of the arms of the macromolecule. The latter in turn is considered to be long enough so that a continuum description of the chain is applicable. To illustrate the effect of the structure of the macromolecule on the escape process a star polymer is used. The Rouse-Ham model is used to calculate exactly the rate of the barrier crossing using multidimensional Kramers theory. The activation energy is found to be linearly dependent on the total number of segments in the star chain. However the preexponential factor depends upon the architecture of the macromolecule. The prefactor is found to increase exponentially with the radius of gyration. The study significantly enhances the understanding of interesting and relevant features of thermally activated processes of soft, complex systems. This could lead to the development of electrophoretic methods for separation of macromolecules of different architectures. It could also help in synthesis of novel materials for controlled drug release for use in therapeutics and novel microreactors.

ACKNOWLEDGMENTS

I thank Professor H. Watanabe, Professor K. L. Sebastian, Professor B. Dünweg, Professor K. Kremer and Dr. Vakhtang Rostiashvili for helpful discussions. I thank JSPS (Post-Doctoral Research Program P01279), and Max-Planck Society for generous financial support.

[1] J.-L. Viovy, Rev. Mod. Phys. **72**, 813 (2000).
[2] D. Rodband and A. Chrambach, Proc. Natl. Acad. Sci. U.S.A. **65**, 970 (1970).
[3] L. S. Lerman and H. L. Frisch, Biopolymers **21**, 995 (1982).
[4] O. J. Lumpkin, P. Dejardin, and B. H. Zimm, Biopolymers **24**, 1573 (1982).
[5] G. W. Slater and J. Noolandi, Biopolymers **25**, 431 (1986).
[6] L. Liu, P. Li, and S. A. Asher, Nature (London) **397**, 141 (1999).
[7] J. Han, S. W. Turner, and H. G. Craighead, Phys. Rev. Lett. **83**, 1688 (1999); J. Han and H. G. Craighead, Science **288**, 1026 (2000); J. Han and H. G. Craighead, Anal. Chem. **74**, 394 (2002).
[8] M. Streek, F. Schmid, T. T. Duong, and A. Ros, J. Biotechnol. **112**, 79 (2004); M. Streek, F. Schmid, T. T. Duong, D. Anselmetti, and A. Ros, Phys. Rev. E **71**, 011905 (2005).
[9] F. Tessier and G. W. Slater, Appl. Phys. A: Mater. Sci. Process. **75**, 285 (2002); F. Tessier, J. Labrie, and G. W. Slater, Macromolecules **35**, 4791 (2002).
[10] C. R. Cantor and P. R. Schimmel, *Biophysical Chemistry III: The Behaviour of Biological Macromolecules* (W.H. Freeman and Company, San Francisco, 1980).
[11] D. L. Nelson and M. M. Cox, *Leninger Principles of Biochemistry* (W.H. Freeman and Company, New York, 2005).
[12] K. D. Cole, C. M. Tellez, and R. W. Blakesley, Electrophoresis **21**, 1010 (2000).
[13] E. S. Yeung, Annu. Rev. Phys. Chem. **55**, 97 (2004).
[14] K. L. Sebastian and A. K. R. Paul, Phys. Rev. E **62**, 927 (2000).
[15] H. A. Kramers, Physica (Utrecht) **7**, 284 (1940).
[16] J. S. Langer, Ann. Phys. (N.Y.) **54**, 258 (1969).
[17] P. Hänggi, P. Talkner, and M. Borkovec, Rev. Mod. Phys. **62**, 251 (1990).
[18] V. I. Mel'nikov, Phys. Rep. **209**, 1 (1991).
[19] J. S. Ham, J. Chem. Phys. **26**, 625 (1957).
[20] H. Watanabe, H. Yoshida, and T. Kotaka, Polym. J. (Tokyo, Jpn.) **22**, 153 (1990).
[21] K. L. Sebastian, Phys. Rev. E **61**, 3245 (2000); K. L. Sebas-

tian, J. Am. Chem. Soc. **122**, 2972 (2000).
[22] A. Y. Grosberg and A. R. Khokolov, *Statistical Physics of Macromolecules* (American Institute of Physics, New York, 1994).
[23] S. K. Lee and W. Sung, Phys. Rev. E **63**, 021115 (2001); K. Lee and W. Sung, Phys. Rev. E **64**, 041801 (2001).
[24] M. Doi and S. F. Edwards, *The Theory of Polymer Dynamics* (Clarendon, Oxford, 1986).
[25] Note that the center of the star chain is modeled as a massless, frictionless point. The integration does not cover this point because it has been included in the model as a boundary condition; see Eqs. (4)–(7).
[26] A similar situation also arises in Ref. [23]. They attribute it to the neglect of the quartic part of the potential and show how to overcome this divergence.
[27] H. Yamakawa, *Modern Theory of Polymer Solutions* (Harper and Row, New York, 1971).
[28] J. Samuel and S. Sinha, Phys. Rev. Lett. **90**, 098305 (2003).